Effective connectivity in target stimulus processing: A dynamic causal modeling study of visual oddball task

Milan Brázdil,[a,*] Michal Mikl,[a,b] Radek Mareček,[a] Petr Krupa,[c] Ivan Rektor,[a]

[a]*1st Department of Neurology, St. Anne's University Hospital, Brno, Czech Republic*
[b]*Faculty of Electrical Engineering and Communication, Brno University of Technology, Czech Republic*
[c]*Department of Neuroimaging, St. Anne's University Hospital, Brno, Czech Republic*

Purpose: To investigate the fundamental connectivity architecture of neural structures involved in the goal-directed processing of target events.
Methods: Twenty healthy volunteers underwent event-related functional magnetic resonance imaging (fMRI) while performing a standard oddball task. In the task, two types of visual stimuli – rare (target) and frequent – were randomly presented, and subjects were instructed to mentally count the target stimuli. Dynamic causal modeling (DCM), in combination with Bayes factors was used to compare competing neurophysiological models with different intrinsic connectivity structures and input regions within the network of brain regions underlying target stimulus processing.
Results: Conventional analysis of fMRI data revealed significantly greater activation in response to the target stimuli (in comparison to the frequent stimuli) in several brain regions, including the intraparietal sulci and supramarginal gyri, the anterior and posterior cingulate gyri, the inferior and middle frontal gyri, the superior temporal sulcus, the precuneus/cuneus, and the subcortical grey matter (caudate and thalamus). The most extensive cortical activations were found in the right intraparietal sulcus (IPS), the anterior cingulate cortex (ACC), and the right lateral prefrontal cortex (PFC). These three regions were entered into the DCM. A comparison on a group level revealed that the dynamic causal models in which the ACC and alternatively the IPS served as input regions were superior to a model in which the PFC was assumed to receive external inputs. No significant difference was observed between the fully connected models with ACC and IPS as input regions. Subsequent analysis of the intrinsic connectivity within two investigated models (IPS and ACC) disclosed significant parallel forward connections from the IPS to the frontal areas and from the ACC to the PFC and the IPS.
Conclusion: Our findings indicate that during target stimulus processing there is a bidirectional frontoparietal information flow, very likely reflecting parallel activation of two distinct but partially overlapping attentional or attentional/event-encoding neural systems. Additionally, a simple hierarchy within the right frontal lobe is suggested with the ACC exerting influence over the PFC.
© 2006 Elsevier Inc. All rights reserved.

Keywords: fMRI; Target detection; Oddball paradigm; Connectivity; Dynamic causal modeling

Introduction

Information processing in the human brain is based on two fundamental principles: functional specialization and functional integration. The first emphasizes the specialization of functions within different brain areas; the latter stresses the fact that function also emerges from the flow of information between involved brain areas (Ramnani et al., 2004). While functional brain mapping has been extensively used in the last decade to detect what cerebral regions are specialized for specific functions, functional integration studies are continuing to emerge. They primarily aim to describe how functionally specialized areas interact and how these interactions depend on changes of context (Friston et al., 2003; Penny et al., 2004a).

Functional integration studies make use of the concept of "effective connectivity", defined as the influence one neural system exerts over another. In contrast to simple "functional connectivity", it is context-dependent, and it provides information about the directionality of functional relations between activated brain areas. Analyses of effective connectivity are based on statistical models that make anatomically motivated assumptions and restrict their inferences to networks comprising a number of preselected regions. These analyses are hypothesis-driven rather than data-driven, and are most applicable when one has knowledge of the relevant functional areas (e.g., from analyses of functional specialization).

There are several approaches to modeling effective connectivity from functional MRI data. The superiority of dynamic causal

* Corresponding author. Fax: +420 543 182 624.
  E-mail address: mbrazd@med.muni.cz (M. Brázdil).

  Available online on ScienceDirect (www.sciencedirect.com).

modeling (DCM) over other existing approaches is mainly demonstrated by the fact that it has been designed specifically for the analyses of fMRI time-series (Friston et al., 2003). The basic distinction is that DCM uses a "forward model" of how neuronal or synaptic activity is transformed into a measured hemodynamic response. This enables the parameters of a neuronal model (i.e., effective connectivity is parametrized here in terms of coupling) to be estimated from observed data. DCM employs an explicit generative model of measured brain responses that embraces their nonlinear and dynamic nature. In DCM, designed experimental inputs may elicit responses through direct influences on specific anatomical nodes, or they may affect the system by inducing changes in coupling among brain areas. The aim of DCM is to estimate, and make inferences about, coupling and how that coupling is influenced by changes in experimental context. It is used to test the specific hypothesis that motivated the experimental design. Thus the results are specific to the task and stimuli employed during the experiment.

One of the most widely utilized experimental paradigms in cognitive neuroscience is the oddball task, which has been used extensively to study task-relevant and goal-directed stimulus processing in the human brain. It is a simple discrimination task with a randomly alternating presentation of two types of sensory stimuli: one frequent and one rare. The subject performing the oddball task is instructed to ignore frequent (standard) stimuli and to detect rare (target) stimuli. In the subject's averaged electroencephalogram (EEG), a large long-latency positive waveform known as a P3 component of event-related potentials (ERP) is typically observed 300–500 ms after the target stimuli, while an analogous response is virtually absent after the standard stimuli. This conspicuous P3 potential is generally viewed as reflecting decision-making or cognitive closure of the recognition processing (Verleger, 1988). It has mostly been linked to both orienting and memory mechanisms (Squires et al., 1975; Paller et al., 1987). Some more recent evidence nevertheless clearly supports the idea that P3 is actually a much more complex phenomenon, reflecting a number of related cognitive processes including decision making and the assessment of stimulus relevance (Andreassi, 1995). In addition to stimulus-related processing, it certainly reflects response-related processing (Verleger, 1997; Brázdil et al., 2003a). Difficulties with the interpretation of P3 phenomenon seem to be closely related to its complexity. P3 can be further subdivided into a frontal P3a, which is relatively enhanced by non-target rare and by novel (distractor) stimuli in an extended oddball task (three types of stimuli-target, standard, and distractor), and a later parietal P3b, enhanced by certainty of target detection (Squires et al., 1975; Snyder and Hillyard, 1976). The P3a then seems to reflect the orienting response (attentional function), while P3b has been suggested to embody the closure of the cognitive event-encoding cycle (Halgren et al., 1998). The most recent evidence suggests that parietal P3b may reflect a whole set of processes that mediate between perceptual analysis and response initiation (Verleger et al., 2005).

To investigate what brain regions are specialized in task-relevant and goal-directed (target) stimulus processing within the oddball task, many electrophysiological and hemodynamic studies have been performed. Previous ERP studies using electrodes implanted in the human brain unequivocally demonstrated multiple generators of P3 potentials in different cortical and subcortical brain structures (Halgren et al., 1980, 1995a,b, 1998; Yingling and Hosobuchi, 1984; McCarthy et al., 1989; Kiss et al., 1989; Puce et al., 1989, 1991; Kropotov and Ponomarev, 1991; McCarthy, 1992; Baudena et al., 1995; Seeck et al., 1995; Brázdil et al., 1999, 2001; Rektor et al., 2003, 2004). However, a complete list of them has yet to be determined. With the availability of modern imaging technologies, event-related fMRI (efMRI) has been repeatedly used over the past years to seek the neural sources of ERPs and to consequently determine the brain regions involved in a target detection (McCarthy et al., 1997; Menon et al., 1997; Yoshiura et al., 1999; Opitz et al., 1999; Linden et al., 1999; Kirino et al., 2000; Clark et al., 2000; Stevens et al., 2000; Kiehl et al., 2001; Strange and Dolan, 2001; Ardekani et al., 2002; Brázdil et al., 2003b; Mulert et al., 2004). The relatively homogenous findings from various authors with a detection of significant hemodynamic changes within most brain regions that have been known from intracerebral measurements (the anterior and posterior cingulate gyri, superior and inferior parietal lobules, supramarginal gyri, precentral gyri, lateral prefrontal and temporal cortices, cuneus/precuneus, and the subcortical grey matter-thalamus and caudate) have suggested a high degree of concordance between electrophysiological and hemodynamic responses. At the same time, however, some significant discrepancies between the efMRI data and the results of previously published intracranial ERP studies have been revealed. Hemodynamic studies have very rarely revealed any post-target activation within the mesiotemporal structures even though hippocampal formation is now widely accepted as a powerful generator of P3 activity. Similarly, some discrepancies can be seen between fMRI and ERP data from dorsolateral prefrontal cortex; this region is strongly activated by targets (not novels) in fMRI studies while P3 directly recorded from this structure is relatively enhanced by non-target rare and novel stimuli. And finally a more spatially extensive genesis of P3 potential has been proven within the anterior cingulate gyrus (ACC) in intracerebral ERP studies. Similar incongruities were also detected by a recently published combination of an event-related fMRI and an intracerebral ERP study of auditory oddball task performed on the same subjects (Brázdil et al., 2005).

In contrast to the advanced investigation of functional specialization during target stimulus processing, practically nothing is yet known about related functional integration. It was therefore the aim of this study to investigate the connectivity pattern subserving the goal-directed target stimulus processing during an oddball task. We used event-related fMRI combined with the above-introduced dynamic causal modeling. In this study, DCM enables inferences on the parameters representing influences of experimentally designed inputs and on the intrinsic coupling of different brain regions. Given the lack of knowledge on the connectivity between brain areas implicated in target stimulus processing, we precluded modulating factors and focused on the investigation of input regions and the intrinsic connectivity pattern. Based on the electrophysiological proof of two anatomically and functionally separated P3 systems-frontal P3a and parietal P3b (Halgren et al., 1998), we hypothesized that we would reveal two different connectivity patterns—one subserving attentional functions (with hypothetical input in the frontal lobe cortical structures) and the second subserving a set of event-encoding processes (with hypothetical input in the parietal areas). The basic premise for this hypothesis was the theoretical involvement of all three selected brain regions (anterior cingulate, lateral prefrontal cortex, and intraparietal sulcus) in both P3 systems.

Methods and materials

Subjects and study design

A total of 20 healthy volunteers (13 females and 7 males) ranging in age from 18 to 33 years (mean age 23 years; median age 22; standard deviation 3.9) participated in the study. All of them were right-handed and had normal vision. Informed consent was obtained from each subject prior to the experiment. The study received the approval of the local ethics committee.

A visual oddball task was performed. In this task, a train of equally spaced visual stimuli is presented to the subjects. There are two types of stimuli: the standard stimuli and the target stimuli. The standard events occur more frequently than the targets. The subjects are instructed to mentally count the target stimuli and report the total number at the end of the experiment. In the present study, the standard visual stimulus (93.7% of trials) was an image consisting of the string of white characters 'OOOOO' on a dark background, while the target image (6.25% of trials) was the string of white characters 'XXXXX' on the same dark background (Ardekani et al., 2002). Visual stimuli were delivered to a projection screen via a data projector and were seen by the subjects through a mirror that was mounted on the MRI scanner's radio frequency head coil. A total of 1024 images were shown to the subjects (64 targets and 960 standards) in four experimental runs of 256 images each. The interstimulus interval was fixed at 1600 ms. The duration of stimuli exposure was constant at 500 ms. During the time in which stimuli were not shown (1100 ms), the screen was dark. The targets were distributed randomly amongst the four runs and 1024 trials.

Image acquisition

Imaging was performed on a 1.5 T Siemens Symphony scanner equipped with Numaris 4 System (MRease). Functional images were acquired using a gradient echo, echoplanar imaging (EPI) sequence: TR (scan repeat time)=1600 ms, TE=45 ms, FOV=250 mm, flip angle=90°, matrix size 64×64, slice thickness=6 mm, 15 transversal slices per scan. The imaged volume covered most of the brain excluding the vertex and including the upper cerebellum. Each functional study consisted of four runs, each run consisted of 256 scans (total 1024 scans per subject). These runs were separated by only a few seconds to obtain the number of counted targets from subjects. The subjects were instructed to stay still during these breaks and to answer only the number of counted targets. Following functional measurements, high-resolution anatomical T1-weighted images were acquired using a 3D sequence that served as a matrix for the functional imaging (160 sagittal slices, resolution 256×256 resampled to 512×512, slice thickness=1.17 mm, TR=1700 ms, TE=3.96 ms, FOV=246 mm, flip angle=15°).

Conventional image analysis

An SPM2 program (Functional Imaging Laboratory, the Wellcome Department of Imaging Neuroscience, Institute of Neurology at University College London, UK) running under Matlab 6.5 (Mathworks Inc., USA) was used to analyze the fMRI data. The following pre-processing was applied to each subject's time-series of fMRI scans: realignment to correct for any motion artifacts; slice timing correction; normalization to fit into a standard anatomical space (MNI); spatial smoothing using a Gaussian filter with a FWHM of 8 mm; high-pass filter with a cut-off at 128 s; and an autoregressive model to estimate serial correlations. The voxel size generated from the above acquisition parameters was oversampled to $3 \times 3 \times 3$ mm. To determine the brain regions that showed significantly greater time-locked activation to targets, a General Linear Model as implemented in SPM2 was used. As a basis set for analysis, a canonical hemodynamic response function (hrf) with time and dispersion derivatives was selected. Statistical parametric maps with *F*-statistic were computed. The analysis of individual subjects was performed at a significance threshold of $P<0.05$ corrected for multiple comparisons. We used random-effect analysis to compute group activation. ANOVA for three groups was used as a second-level statistics (individual t-contrasts were carried out for canonical hrf and its temporal and dispersion derivatives). Group results were calculated at a significance threshold of $P<0.001$ corrected for multiple comparisons controlling FWE.

Dynamic causal modeling

DCM (Friston et al., 2003) as implemented in SPM2 was used to evaluate our hypothesis about effective connectivity during an oddball task. DCM gives us the possibility of making inferences about the influences that one neural system exerts over another and how this is affected by the experimental context. To define the dynamic causal models, we selected three brain regions within the right hemisphere with significantly greater activation after targets: the intraparietal sulcus (IPS), the anterior cingulate cortex (ACC), and the lateral prefrontal cortex (PFC) (for details see Table 1). The definition of these brain regions relied on activation clusters obtained from a conventional analysis of group data. To allow for interindividual differences in the peak locations of brain activations, individual coordinates of these ROIs were found for each subject at the nearest local maximum of the given functional region. Within individual subjects, for DCM purposes, all four of the functional runs were concatenated into one large data set. Prior to concatenation, the effect of discontinuities was checked. No important changes in detected head movements between functional runs were observed after movement correction. No significant differences were observed between activation maps from concatenated and separated data. Functional time-series were extracted from spherical volumes (6 mm radius) and entered into the DCM. The time-series were adjusted with respect to the null space of selected contrast (targets). This means that the null space time-series was subtracted from filtered and whitened time-series and the effect of nuisance variables (for instance, mean signal intensity) and the effect of regressors of no interest were removed. Then, final time-series variations are caused only by the experimental effect of interest. In our case, the effect of interest is composed of regressors for target stimuli (hrf+derivatives). We focused on driving inputs and intrinsic connections only because our oddball paradigm was designed just to determine the effect of target stimuli among frequent events, and it was not possible to use modulatory inputs.

Our approach, similar to the one used by Ethofer et al. (2005), was to construct and assess dynamic causal models. First, we were interested in determining which of the regions was the most likely input region. Fully connected models (with no a priori constraints on their connectivity structure) in which external inputs (target stimuli) were specified to enter the network via one of the selected regions (IPS vs. ACC vs. PFC) were compared. Because of the

Table 1
Brain areas that showed significantly greater activation in response to target stimuli based on an average across 20 subjects

ROI	BA	MNI coordinates (x, y, z)	Number of activated voxels	F-statistics	Z-scores
Frontal lobe					
Middle frontal gyrus R	10, 46	39, 39, 30	272	37.86	7.31
Middle frontal gyrus L	10	−33, 54, 24	75	31.43	6.83
Inferior frontal gyrus R	9	48, 6, 33	235	40.47	7.48
Inferior frontal gyrus L	44, 9	−57, 6, 18	173	39.41	7.41
Precentral gyrus R	6	48, −6, 48	110	28.89	6.63
Precentral gyrus L	6	−48, −9, 48	148	36.97	7.25
Anterior cingulate cortex R	32	9, 21, 36	247	42.52	7.60
Anterior cingulate cortex L	32	−9, 15, 39	169	35.56	7.15
Medial frontal gyrus R	10	0, 54, −6	31	37.29	7.27
Medial frontal gyrus L	10	0, 54, −6	38	37.29	7.27
Parietal lobe					
Intraparietal sulcus R	40, 7	33, −57, 45	242	45.21	7.76
Intraparietal sulcus L	40, 7	−30, −57, 42	103	31.71	6.86
Precuneus R	7	15, −72, 42	112	31.84	6.87
Precuneus L	7	−24, −72, 42	62	26.35	6.39
Posterior cingulate cortex R	30, 31	12, −54, 18	232	39.15	7.39
Posterior cingulate cortex L	30, 31	−9, −57, 18	140	38.09	7.32
Temporal lobe					
Superior temporal sulcus R	21, 22	51, −24, −3	58	29.33	6.66
Middle temporal gyrus R	21	45, −45, 6	186	33.15	6.97
Middle temporal gyrus L	21	−48, −72, 27	19	23.30	6.09
Occipital lobe					
Cuneus R	17, 23	6, −76, 30	100	24.25	6.18
Cuneus L	17, 23	−12, −75, 30	132	28.55	6.59
Middle occipital gyrus L	18, 19	−30, −90, 3	195	32.64	6.93
Others					
Thalamus R		9, −12, 3	107	29.39	6.67
Thalamus L		−9, −12, 0	118	25.92	6.35
Caudate R		12, 6, 3	33	27.86	6.53
Caudate L		−12, 3, 6	93	34.08	7.04

The activations were significant at $P < 0.001$ after correction for multiple spatial comparisons. The brain regions entered into the DCM are highlighted.
ROI, regions of interest; voxel size $3 \times 3 \times 3$ mm.

superiority of two possible inputs (ACC and IPS, see Results for more details) over the third (PFC), and no significant differences between those two, two types of connectivity structure were presumed: the first one with input into the ACC and the other one with input into the IPS. Second, we were interested in determining the intrinsic connectivity pattern involved in target stimulus processing. Four specific DCM models with different intrinsic connectivity patterns from the input regions and one fully connected DCM model were used. A fully connected model (Model 1) was used with bidirectional connections of all regions. Specific models were constructed with parallel forward connections (Model 2) starting from the input region and with variations of this parallel model according to additional connections among the end regions (Model 3, 4, and 5). All of these types of models were created for each subject. Subsequently, group DCM results were assessed as an average over a number of fitted DCM models. The inferences correspond to a Bayesian fixed effect analysis. These group models with different intrinsic connectivity patterns were compared to each other to find the most appropriate intrinsic connection structure. Model evidence was computed based on Bayesian and Akaikes information criterion (BIC and AIC,

respectively). Model comparison of models $m=1$ and $m=2$ was performed with computing Bayes factors $B_{1,2}$ for group DCMs by

$$B_{1,2} = \frac{P(y|m=1)}{P(y|m=2)}.$$

When Bayes factors are >1, the data favored Model 1 over Model 2; when Bayes factors are <1 then the data favored Model 2. If both AIC and BIC provided Bayes factors of at least e (the natural exponent 2.7183) or less than $1/e$, we regarded this as consistent evidence (for more details, see Penny et al., 2004b). All of the averaging and comparison were performed using SPM2 built functions.

Results

Behavioral data

The satisfactory co-operation of all subjects was observed during the experiment. In most experimental sessions, the subjects reported the number of targets correctly. The mean counting

accuracy (i.e., accuracy of subjects' reports at the end of each run) was 99.3% (±SD 1.08, minimum 96.86).

Conventional fMRI analysis

Significantly greater fMRI activations to target stimuli were found in several brain regions, including the intraparietal sulci and the supramarginal gyri (BA 40,7), the anterior and posterior cingulate gyri (BA 32,31,30), the medial, inferior and middle frontal gyri (BA 9,10,44,46), the precentral gyri (BA 6), the superior temporal sulcus and the middle temporal gyri (BA 21), the precuneus (BA 7), the cuneus (BA 17,23), and the subcortical grey matter (thalamus and caudate). Most of the activations were bilateral; however, obvious right-sided predominance was observed in most of the activated regions. The largest and most consistent cortical activations were revealed within the right intraparietal sulcus, the right anterior cingulate area, and the right lateral prefrontal cortex (namely the middle frontal gyrus—BA 10 and 46). Table 1 summarizes the anatomical areas, their MNI coordinates, the number of voxels with significantly greater activation to target stimuli compared to frequent stimuli, F-statistics, and Z-scores ($P < 0.001$, corrected). Fig. 1 presents related composite maps.

Dynamic causal modeling

The mean signal intensities in the three brain regions entered into the DCM were 496±36.9, 476±31.3, 419±44.3 in the right IPS, ACC, and right PFC, respectively (mean±standard deviation; arbitrary units).

Fully connected dynamic causal models with driving inputs in the ACC and IPS were significantly superior to a fully connected alternative model in which PFC was defined as the input region ($B_{IPS,PFC} = 4.00$; $B_{ACC,PFC} = 7.06$). At the same time, no significant differences were found between models with IPS and alternatively ACC as input regions, although the model with ACC as the input region was slightly superior ($B_{ACC,IPS} = 1.76$).

Five different DCMs for both IPS and ACC as input regions were compared to investigate intrinsic connectivity patterns within the selected brain regions (Fig. 2). The resulting Bayes factors for models with ACC or IPS as input regions are summarized in Tables 2 or 3, respectively. We can see that the fully connected model (Model 1) is significantly inferior if compared to all other models. The simple parallel model (Model 2) seems to be the most probable structure of intrinsic connections for both ACC and IPS as input regions. Although its superiority over other models is not always significant, this model has the highest Bayes factors and the most or equal number of significant comparisons.

Discussion

In performing a simple oddball task, at least two distinct neurocognitive networks are activated-the network for directed attention (or less specifically top-down attentional-control processes) and the network for selective processing of target stimuli. It has been repeatedly suggested that directed attention is organized at the level of a distributed large-scale network revolving around three cortical epicenters (or local networks): the dorsolateral prefrontal cortex, the anterior cingulate, and the posterior parietal cortex (Mesulam, 1981, 1990, 1999; Nebel et al., 2005). At the same time, however, each of these brain regions very likely provides slightly different but interactive and complementary types of attentional function. Their exact role in alertness, orienting, and executive control is a continuing source of debate (MacDonald et al., 2000; Luks et al., 2002; Corbetta and Shulman, 2002; Milham et al., 2003; Kondo et al., 2004; Fan et al., 2005; Konrad et al., 2005). A more detailed analysis of intracerebral P3 phenomena indeed enabled the differentiation of the two brain systems that are activated during an oddball task and that produce a P3 potential. The first of them – a frontoparietocingulate system – generates a P3a; the generators were consistently observed in the dorsolateral prefrontal cortex, the anterior and posterior cingulate cortex, the inferior parietal cortex (including anterior part of the IPS), and some temporal sites including the parahippocampal gyrus. This system has been
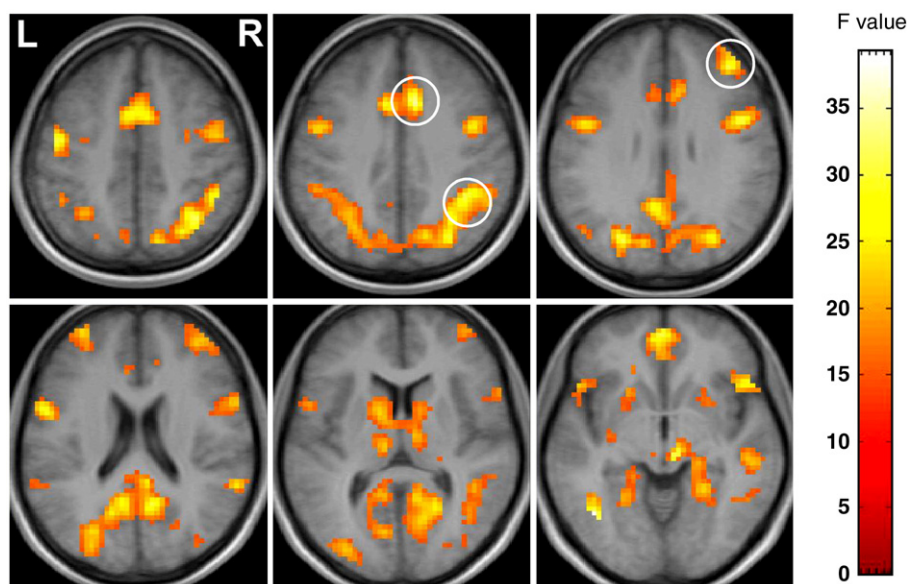

Fig. 1. Composite maps of 20 subjects showing brain regions responsive to the target stimuli ($P < 0.001$ corrected). Statistical parametric maps of the F ratio, based upon a conventional SMP analysis. Regions of interest are indicated by white circles.
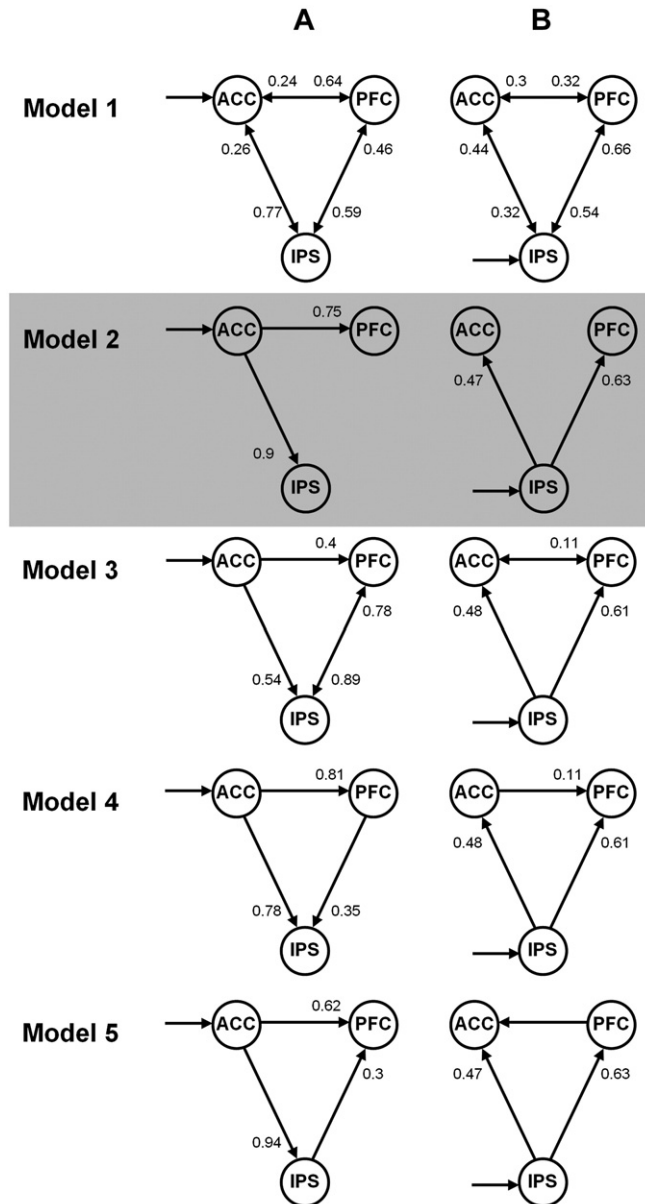
Fig. 2. Hypothetical intrinsic connectivity structure of dynamic causal models for driving input connected both in ACC (left column/A/of DCMs) and IPS (right column/B/of DCMs) regions. Model 1 = fully connected model, Model 2 = parallel forward connection, Models 3, 4, and 5 = variants on parallel connected model with additional connections between the end regions. Intrinsic connections are shown as directed black arrows. Significant connection strengths (at 95% confidence) are reported alongside. A missing number means that a specific connection is not significantly greater than a threshold of 0 Hz. The most probable structure of intrinsic connections is highlighted.

associated with the attentional functions. The second system associated with a later P3b may envelope cognitive contextual integration, possibly also with some components of attention. It engages the ventrolateral prefrontal cortex, the superior temporal sulcus, the hippocampus, and the posterior parietal cortex (intraparietal sulcus and its vicinity) (Halgren et al., 1998). Some recent neuroimaging studies have also demonstrated distinct networks for top-down attentional-control processes and subsequent

selective processing of target stimuli, even if their results are less clearly consistent (Opitz et al., 1999; Kirino et al., 2000; Clark et al., 2000; Hopfinger et al., 2000, 2001; Kiehl et al., 2001). Generally, fMRI data confirm a certain degree of anatomical independence of these two functional systems, but at the same time the data have revealed a common activation within IPS bilaterally and right PFC associated with both the target (P3b) and distractor conditions (P3a) (Bledowski et al., 2004a,b). It seems therefore that there is a substantial overlap for both P3a and P3b systems, similar to the overlap that has been proven for different attentional functions (Corbetta and Shulman, 2002; Fan et al., 2005). As anticipated, our results of conventional fMRI analysis revealed the most extensive activation after target stimuli in the right posterior parietal cortex (namely within the intraparietal sulcus, in both its anterior and posterior part), the right lateral prefrontal cortex, and the anterior cingulate. These findings are fully in agreement with the results of previously performed fMRI studies on oddball tasks, hemispheric differences inclusive (Stevens et al., 2005). The one component of the posterior parietal cortex that is most consistently activated in all attentional tasks lies within the banks of the IPS and its immediate vicinity. The banks of the IPS thus constitute the parietal core of the attentional network in the human brain, although the adjacent parts of the inferior, superior and medial parietal lobules are also likely to participate in the integration of related neural activities (Gitelman et al., 1999; Mesulam, 1999). From this viewpoint, it seemed reasonable to estimate, and to make inferences about, the coupling among IPS, ACC, and PFC during target processing.

Dynamic causal modeling used in this study clearly revealed a superiority of DCMs in which ACC, and alternatively IPS, served as input regions as compared to a model in which PFC was assumed to receive external inputs. The fact that no significant difference was observed between fully connected models with ACC and IPS as input regions may reflect the parallel involvement of two neuronal circuits – "frontal" (P3a system for top-down attentional control) and "parietal" (P3b attentional/event encoding system) – with their balanced and complementary roles in target detection. In agreement with this hypothesis, a further analysis of intrinsic connections disclosed highly significant coupling among the selected brain areas in both ACC and IPS dynamic causal models. With respect to the intrinsic connectivity structure, various models for target detection were compared. Comparison of the models based on their evidence as computed by a Bayesian approach revealed a superiority of simple parallel models over the fully connected models and other models with additional connections between the end regions. These findings strongly suggest changes in connectivity among IPS, ACC, and PFC induced by targets. Our study further allows the claim that targets induce bidirectional coupling between the frontal and parietal regions. A simple hierarchy of forward connections within the right frontal lobe is also suggested, with ACC exerting influence over PFC. Interestingly similar findings were obtained from some previously published experiments on attention and execution, even if these were performed with other approaches. For example in a recent paper of Luks et al. (2002) the involvement of the ACC in monitoring the preparatory allocation of attention for conflict and the role of the PFC in holding cognitive goals in working memory and allocating attention to the appropriate processing systems to meet these goals, is quite congruently suggested. Elsewhere, the ACC was repeatedly suggested as the central coordinating structure in an "executive attention" network (Fernandez-Duque and Posner, 2001; Fan et al., 2005; Mottaghy et al., 2006). Other studies, however, supported the model that the PFC is responsible for

Table 2
Bayes factors for comparing models with different intrinsic connectivity pattern when external input (target stimuli) is specified to enter the network via the ACC

	Model 1	Model 2	Model 3	Model 4	Model 5
Model 1		$B_{2,1} = 53.37$	$B_{3,1} = 15.68$	$B_{4,1} = 32.81$	$B_{5,1} = 22.12$
Model 2	$B_{1,2} = 0.018$		$B_{3,2} = 0.293$	$B_{4,2} = 0.614$	$B_{5,2} = 0.414$
Model 3	$B_{1,3} = 0.063$	$B_{2,3} = 3.402$		$B_{4,3} = 2.091$	$B_{5,3} = 1.410$
Model 4	$B_{1,4} = 0.030$	$B_{2,4} = 1.626$	$B_{3,4} = 0.478$		$B_{5,4} = 0.674$
Model 5	$B_{1,5} = 0.045$	$B_{2,5} = 2.412$	$B_{3,5} = 0.709$	$B_{4,5} = 1.483$	

The lower Bayes factor from AIC and BIC factors is presented. Significant and consistent findings are highlighted. Model 1 = fully connected model, Model 2 = parallel forward connection, Models 3, 4, and 5 = variants on parallel connected model with additional connections between the end regions.

preparatory attention, and the ACC monitors for conflict during later stages of stimulus processing and response selection (MacDonald et al., 2000; Hopfinger et al., 2000). It seems therefore extremely problematic to compare our findings with the results of previously published experiments on different attentional or executive paradigms (including studies on error and conflict).

Certainly it would be no less interesting to also investigate the role of other areas (e.g., the insular cortex, posterior cingulate, superior temporal sulcus, cuneus/precuneus, etc.) in target stimulus processing. Actually much less is known about the contribution of these brain regions to the executive functions. Unfortunately, however, the methodology used in this study is substantially limited in understanding 'whole brain' effective connectivity. DCM is typically used to test the specific hypothesis that motivated the experimental design. It is not an exploratory technique; this method is hypothesis driven rather than data driven (Friston et al., 2003; Penny et al., 2004a). It was therefore essential to select regions that are both unambiguously involved in the same cognitive processing and in which effective connectivity can be reasonable hypothesized. All of three selected regions are well-known and powerful generators of P3 potential and thus they are clearly involved in the oddball task. They were consistently activated across the subjects and in group data they were activated most extensively of all the activated brain regions. And finally we were able to formulate a specific hypothesis based on the previously published data (even though contradictory to some extent and related to other attentional paradigms; as far as we are aware no connectivity study has been published on a specific oddball task). In contrast, any hypothesis on effective connectivity between other brain areas (e.g., the insula-posterior cingulate or insula-PFC) would be extremely speculative and the use of DCM might provide us with confusing results. Another reason for excluding the insula, posterior cingulate cortex or further activated brain regions from DCM analysis was the problem of indicating individual coordinates of these ROIs in some subjects. Actually there were less consistent findings in the regions outside the ACC, PFC, and IPS during the performed task, which prevented reasonably indicating all ROIs for some subjects.

The results of this DCM study confirm the presumed cooperation of ACC, PFC, and IPS during target detection. There is no doubt that all these brain regions are at least partially involved in top-down attentional control processing. From this viewpoint, the role of ACC seems to be crucial. This cortical structure is very likely involved in different attentional functions (i.e., alertness, orienting, attention shifting, monitoring and executive control, etc.) and at the same time it represents a powerful source of P3a, the latency of which is significantly shorter here than in parietal cortical structures. Thus DCM with ACC as a driving input and forward parallel connections to PFC and IPS most likely represents a top-down attentional control system, in which ACC (activated by targets) modulates an activity in the right PFC and IPS. In agreement, Kondo et al. (2004) recently demonstrated that activation of task-dependent posterior regions is regulated by the top-down control of the ACC.

In contrast, significant dynamic causal model with IPS as a driving input and parallel forward connections from IPS to the frontal regions may reflect either later stages of attentional processing or subsequent selective processing of target stimuli. In both situations, this model can be viewed as a P3b analogue. Targets entering IPS are very likely able to modulate an activity within ACC and PFC. The secondary involvement of ACC may reflect a monitoring stimulus processing or an initiation of task-related response to targets (Luks et al., 2002). This two-stage activation of ACC is congruent with the anatomical properties of ACC as well as with the typical overlap of a different functional domain in this cortical structure that distinguishes ACC from other frontal regions (Paus, 2001).

Conclusion

Using dynamic causal modeling, we investigated the fundamental connectivity architecture of neural structures involved in target detection. Our findings revealed significant target-induced changes in connectivity among the right intraparietal sulcus, the anterior cingulate cortex, and the right prefrontal cortex. Our data

Table 3
Bayes factors for comparing models with different intrinsic connectivity pattern when external input (target stimuli) is specified to enter the network via the IPS

	Model 1	Model 2	Model 3	Model 4	Model 5
Model 1		$B_{2,1} = 71.53$	$B_{3,1} = 10.54$	$B_{4,1} = 31.02$	$B_{5,1} = 26.73$
Model 2	$B_{1,2} = 0.014$		$B_{3,2} = 0.147$	$B_{4,2} = 0.433$	$B_{5,2} = 0.373$
Model 3	$B_{1,3} = 0.094$	$B_{2,3} = 6.781$		$B_{4,3} = 2.941$	$B_{5,3} = 2.534$
Model 4	$B_{1,4} = 0.032$	$B_{2,4} = 2.305$	$B_{3,4} = 0.340$		$B_{5,4} = 0.861$
Model 5	$B_{1,5} = 0.037$	$B_{2,5} = 2.676$	$B_{3,5} = 0.394$	$B_{4,5} = 1.160$	

The lower Bayes factor from AIC and BIC factors is presented. Significant and consistent findings are highlighted. Model 1 = fully connected model, Model 2 = parallel forward connection, Models 3, 4, and 5 = variants on parallel connected model with additional connections between the end regions.

further indicated that during target stimulus processing there is a bidirectional coupling between the frontal and parietal regions. Additionally, a key role of the anterior cingulate in top-down attentional-control processes was suggested with the ACC exerting influence over the right PFC.

References

Andreassi, J.L., 1995. Psychophysiology: Human Behaviour and Physiological Response, 3rd ed. Lawrence Erlbaum, Hillsdale, NJ.

Ardekani, B.A., Choi, S.J., Hossein-Zadeh, G., Porjesz, B., Tanabe, J.L., Lim, K.O., Bilder, R., Helpern, J.A., Begleiter, H., 2002. Functional magnetic resonance imaging of brain activity in the visual oddball task. Cogn. Brain Res. 14, 347–356.

Baudena, P., Halgren, E., Heit, G., Clarke, J.M., 1995. Intracerebral potentials to rare target and distractor auditory and visual stimuli: III. Frontal cortex. Electroencephalogr. Clin. Neurophysiol. 94, 251–264.

Bledowski, C., Prvulovic, D., Goebel, R., Zanella, F.E., Linden, D.E.J., 2004a. Attentional systems in target and distractor processing: a combined ERP and fMRI study. NeuroImage 22, 530–540.

Bledowski, C., Prvulovic, D., Hoechstetter, K., Scherg, M., Wibral, M., Goebel, R., Linden, D.E.J., 2004b. Localizing P300 generators in visual target and distractor processing: a combined event-related potential and functional magnetic resonance imaging study. J. Neurosci. 24 (42), 9353–9360.

Brázdil, M., Rektor, I., Dufek, M., Daniel, P., Jurák, P., Kuba, R., 1999. The role of frontal and temporal lobes in visual discrimination task-depth ERP studies. Neurophysiol. Clin. 29, 339–350.

Brázdil, M., Rektor, I., Daniel, P., Dufek, M., Jurák, P., 2001. Intracerebral event-related potentials to subthreshold target stimuli. Clin. Neurophysiol. 112/4, 650–661.

Brázdil, M., Roman, R., Daniel, P., Rektor, I., 2003a. Intracerebral somatosensory event-related potentials: effect of response type (button pressing versus mental counting) on P3-like potentials within the human brain. Clin. Neurophysiol. 114, 1489–1496.

Brázdil, M., Dobšík, M., Pažourková, M., Krupa, P., Rektor, I., 2003b. Importance of functional MRI for evaluation of cognitive processes in the human brain. Localization of neuronal populations activated by oddball task. Ces. Slov. Neurol. Neurochir. 1, 20–30.

Brázdil, M., Dobšík, M., Mikl, M., Hluštík, P., Daniel, P., Pažourková, M., Krupa, P., Rektor, I., 2005. Combined event-related fMRI and intracerebral ERP study of an auditory oddball task. NeuroImage 26/1, 285–293.

Clark, V.P., Fannon, S., Lai, S., Benson, R., Bauer, L., 2000. Responses to rare visual target and distractor stimuli using event-related fMRI. J. Neurophysiol. 83, 3133–3139.

Corbetta, M., Shulman, G.L., 2002. Control of goal-directed and stimulus-driven attention in the brain. Nat. Rev., Neurosci. 3 (3), 201–215.

Ethofer, T., Anders, S., Erb, M., Herbert, C., Wiethoff, S., Kissler, J., Grodd, W., Wildgruber, D., 2005. Cerebral pathways in processing of affective prosody: a dynamic causal modeling study. NeuroImage 30, 580–587.

Fan, J., McCandliss, B.D., Fossella, J., Flombaum, J.I., Posner, M.I., 2005. The activation of attentional networks. NeuroImage 26, 471–479.

Fernandez-Duque, D., Posner, M.I., 2001. Brain imaging of attentional networks in normal and pathological states. J. Clin. Exp. Neuropsychol. 23, 74–93.

Friston, K.J., Harrison, L., Penny, W., 2003. Dynamic causal modelling. NeuroImage 19, 1273–1302.

Gitelman, D.R., Nobre, A.C., Parrish, T.B., LaBar, K.S., Kim, Y.H., Meyer, J.R., Mesulam, M.M., 1999. A large-scale distributed network for covert spatial attention: further anatomical delineation based on stringent behavioural and cognitive controls. Brain 122, 1093–1106.

Halgren, E., Squires, N.K., Wilson, C.L., Rohrbaugh, J.W., Babb, T.L., Crandal, P.H., 1980. Endogenous potentials generated in the human hippocampal formation and amygdala by infrequent events. Science 210, 803–805.

Halgren, E., Baudena, P., Clarke, J.M., Heit, G., Liégeois, C., Chauvel, P., et al., 1995a. Intracerebral potentials to rare target and distractor auditory and visual stimuli: I. Superior temporal plane and parietal lobe. Electroencephalogr. Clin. Neurophysiol. 94, 191–220.

Halgren, E., Baudena, P., Clarke, J.M., Heit, G., Marinkovic, K., Deveaux, B., et al., 1995b. Intracerebral potentials to rare target and distractor auditory and visual stimuli: II. Medial, lateral and posterior temporal lobe. Electroencephalogr. Clin. Neurophysiol. 94, 229–250.

Halgren, E., Marinkovic, K., Chauvel, P., 1998. Generators of the late cognitive potentials in auditory and visual oddball tasks. Electroencephalogr. Clin. Neurophysiol. 106, 156–164.

Hopfinger, J.B., Buonocore, M.H., Mangun, G.R., 2000. The neural mechanisms of top-down attentional control. Nat. Neurosci. 3 (3), 284–291.

Hopfinger, J.B., Woldorff, M.G., Fletcher, E.M., Mangun, G.R., 2001. Dissociating top-down attentional control from selective perception and action. Neuropsychologia 39, 1277–1291.

Kiehl, K.A., Laurens, K.R., Duty, T.L., Forster, B.B., Liddle, P.F., 2001. Neural sources involved in auditory target detection and novelty processing: an event-related fMRI study. Psychophysiology 38, 133–142.

Kirino, E., Belger, A., Goldman-Rakic, P., McCarthy, G., 2000. Prefrontal activation evoked by infrequent target and novel stimuli in a visual target detection task: an event-related functional magnetic resonance imaging study. J. Neurosci. 20, 6612–6618.

Kiss, I., Dashieff, R.M., Lordeon, P., 1989. A parieto-occipital generator for P300: evidence from human intracranial recordings. Int. J. Neurosci. 49, 133–139.

Kondo, H., Osaka, N., Osaka, M., 2004. Cooperation of the anterior cingulate cortex and dorsolateral prefrontal cortex for attention shifting. NeuroImage 23, 670–679.

Konrad, K., Neufang, S., Thiel, C.M., Specht, K., Hanisch, C., Fan, J., Herpertz-Dahlmann, B., Fink, G.R., 2005. Development of attentional networks: an fMRI study with children and adults. NeuroImage 28, 429–439.

Kropotov, J.D., Ponomarev, V.A., 1991. Subcortical neuronal correlates of component P300 in man. Electroencephalogr. Clin. Neurophysiol. 78, 40–49.

Linden, D.E.J., Prvulovic, D., Formasino, E., Vollinger, M., Zanella, F.E., Goebel, R., et al., 1999. The functional neuroanatomy of target detection: an fMRI study of visual and auditory oddball tasks. Cereb. Cortex 9, 815–823.

Luks, T.L., Simpson, G.V., Feiwell, R.J., Miller, W.L., 2002. Evidence for anterior cingulate cortex involvement in monitoring preparatory attentional set. NeuroImage 17, 792–802.

MacDonald, A.W., Cohen, J.D., Stenger, V.A., Carter, C.S., 2000. Dissociating the role of the dorsolateral prefrontal and anterior cingulate cortex in cognitive control. Science 288, 1835–1838.

McCarthy, G., 1992. Intracranial recordings in humans. Twelfth Annual Carmel Conference, Carmel, CA.

McCarthy, G., Wood, C.C., Williamson, P.D., Spencer, D.D., 1989. Task-dependent field potentials in human hippocampal formation. J. Neurosci. 9, 4253–4260.

McCarthy, G., Luby, M., Gore, J., Goldman-Rakic, P., 1997. Infrequent events transiently activate human prefrontal and parietal cortex as measured by functional MRI. J. Neurophysiol. 77, 1630–1634.

Menon, V., Ford, J.M., Lim, K.O., Glover, G.H., Pfefferbaum, A., 1997. Combined event-related fMRI and EEG evidence for temporal–parietal cortex activation during target detection. NeuroReport 8, 3029–3037.

Mesulam, M.M., 1981. A cortical network for directed attention and unilateral neglect. Ann. Neurol. 10, 309–325.

Mesulam, M.M., 1990. Large-scale neurocognitive networks and distributed processing for attention, language, and memory. Ann. Neurol. 28, 597–613.

Mesulam, M.M., 1999. Spatial attention and neglect: parietal, frontal and cingulate contributions to the mental representation and attentional targeting of salient extrapersonal events. Philos. Trans. R. Soc. Lond. 354, 1325–1346.

Milham, M.P., Banich, M.T., Claus, E.D., Cohen, N.J., 2003. Practice-related effects demonstrate complementary roles of anterior cingulate and prefrontal cortices in attentional control. NeuroImage 18, 483–493.

Mottaghy, F.M., Willmes, K., Horwitz, B., Muller, H.W., Krause, B.J., Sturm, W., 2006. Systems level modeling of a neuronal network subserving intrinsic alertness. NeuroImage 29, 225–233.

Mulert, C., Jager, L., Schmitt, R., Bussfeld, P., Pogarell, O., Moller, H.J., Juckel, G., Hegerl, U., 2004. Integration of fMRI and simultaneous EEG: towards a comprehensive understanding of localization and time-course of brain activity in target detection. NeuroImage 22, 83–94.

Nebel, K., Wiese, H., Stude, P., de Greiff, A., Diener, H.C., Keidel, M., 2005. On the neural basis of focused and divided attention. Cogn. Brain Res. 25, 760–776.

Opitz, B., Mecklinger, A., Von Cramon, D.Y., Kruggel, F., 1999. Combining electrophysiological and hemodynamic measures of the auditory oddball. Psychophysiology 36, 142–147.

Paller, K.A., Kutas, M., Mayes, A.R., 1987. Neural correlates of encoding in an incidental learning paradigm. Electroencephalogr. Clin. Neurophysiol. 67, 360–371.

Paus, T., 2001. Primate anterior cingulate cortex: where motor control drive and cognition interface. Nat. Rev., Neurosci. 2, 417–424.

Penny, W.D., Stephan, K.E., Mechelli, A., Friston, K.J., 2004a. Modelling functional integration: a comparison of structural equation and dynamic causal models. NeuroImage 23, S264–S274.

Penny, W.D., Stephan, K.E., Mechelli, A., Friston, K.J., 2004b. Comparing dynamic causal models. NeuroImage 22, 1157–1172.

Puce, A., Kalnins, R.M., Berkovic, S.F., Donnan, G.A., Bladin, P.F., 1989. Limbic P3 potentials, seizure localization, and surgical pathology in temporal lobe epilepsy. Ann. Neurol. 26, 377–385.

Puce, A., Andrewes, D.G., Berkovic, S.F., Bladin, P.F., 1991. Visual recognition memory. Neurophysiological evidence for the role of temporal white matter in man. Brain 114, 1647–1666.

Ramnani, N., Behrens, T.E.J., Penny, W., Matthews, P.M., 2004. New approaches for exploring anatomical and functional connectivity in the human brain. Biol. Psychiatry 56 (9), 613–619.

Rektor, I., Kaňovský, P., Bareš, M., Brázdil, M., Streitová, H., Klajblová, H., et al., 2003. A SEEG study of ERP in motor and premotor cortices and in the basal ganglia. Clin. Neurophysiol. 114, 463–471.

Rektor, I., Bareš, M., Kaňovský, P., Brázdil, M., Klajblová, H., Streitová, H., Rektorová, I., Sochůrková, D., Kubová, D., Kuba, R., Daniel, P., 2004. Cognitive potentials in the basal ganglia-frontocortical circuits. An intracerebral recording study. Exp. Brain Res. 158, 289–301.

Seeck, M., Schomer, D., Mainwaring, N., Ives, J., Dubuisson, D., Blume, H., et al., 1995. Selectively distributed processing of visual object recognition in the temporal and frontal lobes of the human brain. Ann. Neurol. 37, 538–545.

Snyder, E., Hillyard, S.A., 1976. Long-latency evoked potentials to irrelevant, deviant stimuli. Behav. Biol. 16, 319–331.

Squires, N.K., Squires, K.C., Hillyard, S.A., 1975. Two varieties of long-latency positive waves evoked by unpredictable auditory stimuli in man. Electroencephalogr. Clin. Neurophysiol. 38, 387–401.

Stevens, A.A., Skudlarski, P., Gatenby, J.C., Gore, J.C., 2000. Event-related fMRI of auditory and visual oddball tasks. Magn. Reson. Imaging 18, 495–502.

Stevens, M.C., Calhoun, V.D., Kiehl, K.A., 2005. Hemispheric differences in hemodynamics elicited by auditory oddball stimuli. NeuroImage 26, 782–792.

Strange, B.A., Dolan, R.J., 2001. Adaptive anterior hippocampal responses to oddball stimuli. Hippocampus 11, 690–698.

Verleger, R., 1988. Event-related potentials and cognition: a critique of the context updating hypothesis and an alternative interpretation of the P3. Behav. Brain Sci. 11, 343–427.

Verleger, R., 1997. On the utility of P3 latency as an index of mental chronometry. Psychophysiology 34, 131–156.

Verleger, R., Jaskowski, P., Wascher, E., 2005. Evidence for an integrative role of P3b in linking reaction to perception. J. Psychophysiol. 19 (3), 165–181.

Yingling, C.D., Hosobuchi, Y., 1984. A subcortical correlate of P300 in man. Electroencephalogr. Clin. Neurophysiol. 59, 72–76.

Yoshiura, T., Zhong, J., Shibata, D.K., Kwok, W.E., Shrier, D.A., Numaguchi, Y., 1999. Functional MRI study of auditory and visual oddball tasks. NeuroReport 10, 1683–1688.